
MASSACHUSETTS INSTITUTE OF TECHNOLOGY
10.26 CHEMICAL ENGINEERING PROJECTS LABORATORY

Continuous Flow Reactor Characterization

Corning Advanced-FlowTM Lab Reactor

Team One

John Deely

Isabel Kaspriskie

Rafid Mollah

Faculty Advisor – Professor Klavs Jensen
Internal Consultant – Dr. Victor Schultz
Teaching Assistant – Arie Havasov

Final Report Revision
Submitted: 17 May 2018

Dear Professor Jensen and Jane,

Thank you for all of your comments for revising our final report. We have appreciated all of the feedback we have received this semester.

We did our best to take into account all of the formatting suggestions presented, and we hope all of the hard work going into it is visible. Please note that the PDF has clickable links to various sections within the document, including the table of contents and the table and figure references. The citation format was fixed to follow ACS suggestions of leaving out article titles.

Most of the revisions that you will notice in comparison to the first draft include moving segments of text from one section to another, like from background to methods. We also included more transition material and introductory topic sentences.

Edits were made to improve the clarity of theory and methods. Following Jane's suggestion, we included more of the model numbers of equipment used throughout experiments. We also were careful to include error in our tables and results.

As we encountered issues with the tanks-in-series model and moved to the dispersion model, we explained the issues that arose. Similarly, we discussed the work we began and had to abandon with the bromination reaction. We hope that our suggestions of transitioning to grayscale and attempting more visible reactions is followed in more years of 10.26.

Best,
Team One (John, Isabel, and Rafid)

Contents

1	Introduction	1
2	Background and Theory	3
2.1	Mixing Ability of Heart-Shaped Cells	3
2.2	Effective Heat Transfer Coefficient	4
2.3	Residence Time Distribution of a Single Reactor Plate	6
2.4	Determining Chemical Kinetics	9
3	Experimental Methods	12
3.1	Mixing Ability of Heart-Shaped Cells	12
3.2	Effective Heat Transfer Coefficient	12
3.3	Residence Time Distribution of a Single Reactor Plate	13
3.4	Determining Chemical Kinetics	14
4	Results	15
5	Discussion	20
6	Conclusions and Recommendations	25

List of Figures

1	Geometry of heart-shaped cells	4
2	Simplified heat exchange diagram	5
3	Heat exchanger models	6
4	Nonideality effects on RTD	7
5	Dispersion model	8
6	Tanks-in-series model	9
7	Wittig reaction	10
8	Single-hexcone model of colorspace for HSV	10
9	RTD collection setup	13
10	Flowrates and striations	16
11	Striation close-up	16
12	Experimental tanks-in-series RTD	17
13	Experimental dispersion RTD	18
14	Wittig dilution plates	18
15	Calibration of Wittig reaction	19
16	Damkohler number for Wittig reaction	24
17	Bromination reaction	25

List of Tables

1	Temperatures for heat transfer coefficient determination	17
2	Mixing time	20
3	Tanks-in-series model results	22
4	Dispersion model results	22
5	Rate constants	23

Abstract

Interest in continuous flow reactors in the organic chemistry community is because of the good heat and mass transfer, reduced waste, better safety, and finer control of reactions in microfluidic reactors. This project studied the Corning Advanced-FlowTM Lab Reactor (AFR), a commercial all-in-one continuous flow reactor system. A proprietary AFR reactor plate contains 197 individual heart-shaped cells, a geometry designed to maximize fluid mixing. Using the November 2017 version of transparent glass reactor plates, we characterized the AFR mixing and heat transfer abilities. Colored water experiments showed consistent mixing times on the order of one second, regardless of flowrate. Modeling the AFR as a parallel current heat exchanger and measuring temperature with thermocouples at inlets and outlets of heat exchange fluid and process fluid determined the effective heat transfer coefficient was $0.349 \pm 0.017 \text{ W/K}$. Residence time distribution was measured using colored inlet pulses and a spectrophotometer to determine a vessel dispersion number of $(4.8 \pm 1.1) \times 10^{-3}$, suggesting flow in the AFR is close to a plug flow reactor. The number of theoretical tanks in series was measured using a tanks-in-series model and a dispersion model, giving 72 ± 11 and 107 ± 23 tanks, respectively, further suggesting plug flow behavior. Proprietary image analysis software was developed to analyze kinetic performance of a Wittig intermediate reaction; the reaction was pseudo first order with activation energy of 33.9 kJ/mol and a frequency factor of $3.1 \times 10^4 \text{ s}^{-1}$.

1 Introduction

In the pharmaceutical and fine chemical industries, small quantities of high-value products are typically produced in batch reactors. Batch production methods require additional time for setup and cleaning, extra material ultimately lost to waste, and large laboratory and plant footprints to accommodate storage of intermediate products (1). Replacing batch reactors with continuous flow reactors when designing a process improves process

safety, reduces equipment footprint, and lowers environmental impacts. Without needing to handle as many intermediates in a reaction process, operators of continuous flow systems are able to run reactions previously considered too hazardous (1). Moreover, less solvent is needed in flow to produce the same amount of product made in batch, mitigating environmental and economic concerns. High throughput and automated quality control, which are possible with continuous flow, improve further the economic considerations associated with process design (2).

As the benefits of continuous flow processes become more evident, companies are creating lower-cost flow technology to meet rising industrial demand. The Corning Advanced-FlowTM Lab Reactor (AFR) is one of the commercially available flow reactor systems on the market and it advertises a simple and ready-to-use introduction to the field of flow chemistry for academic labs, start-up ventures, and industrial pilot plants (3). These systems advertise ease of integration into lab workflows, seamless scale-up, and large improvements in efficiency, but as with any young technology, these claims are not supported by measurements in experimental literature (3).

This project tested claims of the AFR's mixing ability with colored water experiments to calculate mixing times at varying flowrates. A parallel current heat exchanger model and temperature measurements were used to calculate an effective heat transfer coefficient. Injections of colored dye and absorbance measurements were used to create residence time distributions to quantify dispersion of molecules throughout the system. Novel image analysis techniques were developed to study kinetics of a Wittig intermediate reaction. The simple camera/AFR setup is presented as a possible new and flexible method of determining kinetic performance of any color-changing reaction, further expanding the benefits of using a Corning AFR.

2 Background and Theory

2.1 Mixing Ability of Heart-Shaped Cells

High mixing rates are desirable in reactors because more intermolecular contact occurs, improving both reaction conversion and selectivity (4). The Reynold's number (Re) is a dimensionless number that compares the ratio of inertial and viscous forces on a fluid and is used to describe mixing in a system.

$$Re = \frac{UD_h\rho}{\mu} \quad (1)$$

$$D_h = \frac{4A_c}{P} \quad (2)$$

High Reynolds numbers (above 4,000) correspond to the best regimes for fluid mixing and would be ideal for high performance reactors, although intermediate Reynolds numbers in the transition regime (between 2,100 and 4,000) are also desirable.

Shown in Fig. 1, the geometry of the AFR reactor plate heart-shaped cells is designed to facilitate rapid mixing. After moving through a narrow throat 1 mm in diameter, fluid hits a baffle, splitting the stream in half and sending the flow back together in a wider segment of the heart. These changes in hydraulic diameter correspond to changes in Re and flow regime (i.e. laminar versus turbulent). A previous Corning AFR two-phase mixing study using hexane and water, completed by Nieves-Remacha *et al.*, found that Reynolds numbers ranged from 460 to 3,700, confirming that fluid flow patterns throughout the reactor vary from laminar to nearly turbulent (5).

To explain the mixing ability to a new user of the AFR, this project calculated mixing times at varying flowrates. Using blue- and yellow-colored water, the heart at which complete mixing occurred was translated to a time of mixing. A single reactor plate has 197 individual hearts and a total volume of 2.7 mL. The total flowrate and heart of

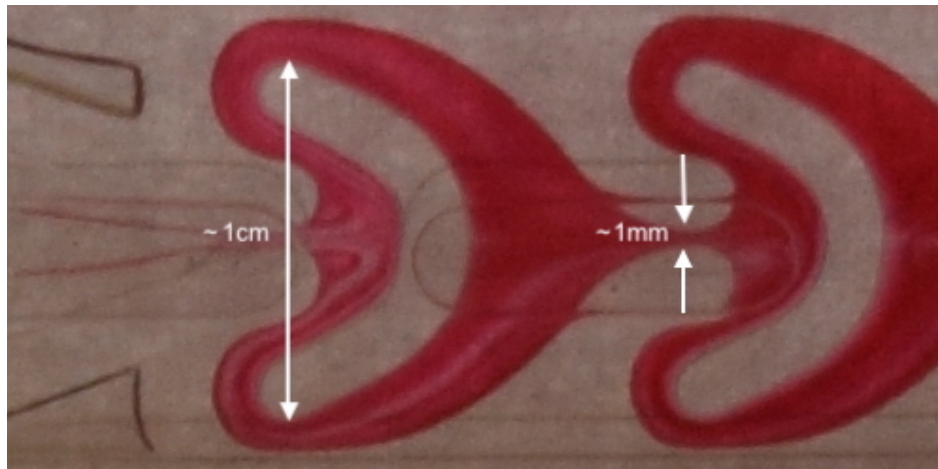


Figure 1: The heart-shaped cells have large changes in cross-sectional area thus Re and flow regime.

completion can be used to calculate mixing time with Eqn. (3).

$$t_{mix} = \frac{V_{total}}{197} \frac{1}{v_o} \quad (3)$$

From Corning's claims, it was expected that mixing time would be short.

2.2 Effective Heat Transfer Coefficient

In reactor design, it is desirable to maximize heat transfer because good heat transfer allows highly exothermic reactions to proceed without excess energy buildup. Flow reactors use small channels with high surface area to volume ratios to increase heat transfer, as seen in Fig. 2. This gives the user the ability to finely tune reaction conditions to improve safety, efficiency, and conversion of products. The Corning AFR brochure advertises 1000x improved heat transfer over batch reactors, a vague claim since batch reactors come in many materials and sizes and thus varying heat transfer capabilities (6). Ignoring Corning's quantitative claims, the qualitative claim of improved heat transfer in the AFR permits easy adjustment of reaction conditions, allowing the user to quickly change the temperature of every fluid particle in the system rather than waiting to heat up the entire vessel. Furthermore, improved heat transfer means highly exothermic reactions can be run

at industrial scales (7). An effective heat transfer coefficient of the AFR is desirable for a user wishing to do safety analysis by calculating temperature increases related to exothermic reactions.

To calculate an effective heat transfer equation, the AFR reactor plate was modeled as a parallel current heat exchanger as in Fig. 2 and Fig. 3. Approximating the reactor plate as a parallel current heat exchanger allowed the use of Eqn. (4) where effective heat transfer coefficient (UA) of the entire system is constrained by experimentally obtained inlet and outlet reactant and thermal fluid temperatures.

$$UA = \frac{\dot{m}C_p(\Delta T_1 - \Delta T_2)}{\Delta T_{lm}} \quad (4)$$

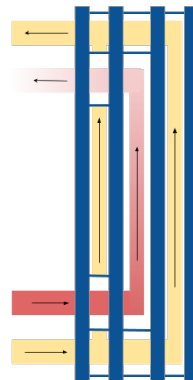


Figure 2: Large area of contact between the heat exchange fluid, the yellow stream, and the process fluid, the red stream, improve heat transfer capabilities of the AFR.

Using parallel current heat exchange is usually undesirable because the temperature difference changes over the length of the unit, as shown in Fig. 3.

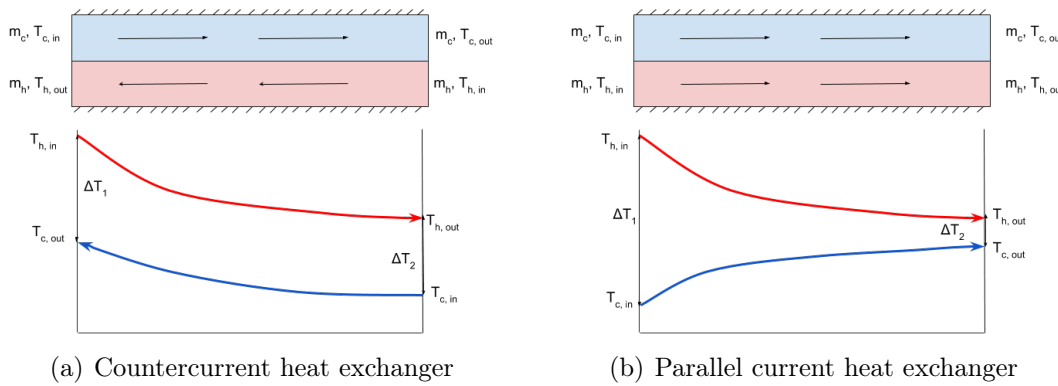


Figure 3: Countercurrent heat exchangers (a) are usually desirable for their continually large ΔT over the unit's length, but for the AFR, parallel current heat exchange (b) is desirable for kinetic performance improvement.

The benefit, however, is that both streams approach the same temperature at the outlet. In the AFR, the inlet process stream should be the desired temperature for the reaction to proceed, but then it needs to be heated or cooled to a safe temperature as it gives off or consumes thermal energy.

2.3 Residence Time Distribution of a Single Reactor Plate

The residence time distribution (RTD) of a reactor is used to describe the system's non-idealities. An RTD is a probability distribution of the amount of time a molecule spends in a flow reactor. In an ideal plug flow reactor (PFR), every molecule spends the same time in the reaction volume, so a sharp peak on the inlet concentration plot would look identical to its outlet concentration plot; however, non-ideal flow patterns in real reactors result in mixing inefficiencies and broaden a sharp inlet peak because molecules do not all spend the same time in the reactor, as shown in Fig. 4.

In this project, both the dispersion model and the tanks-in-series (TIS) model were used to quantitatively compare the AFR to an ideal PFR and describe the broadening effect.

The dispersion model accounts for nonidealities caused by backflow mixing in either the axial or longitudinal direction of flow (8). Age distributions are developed by solving

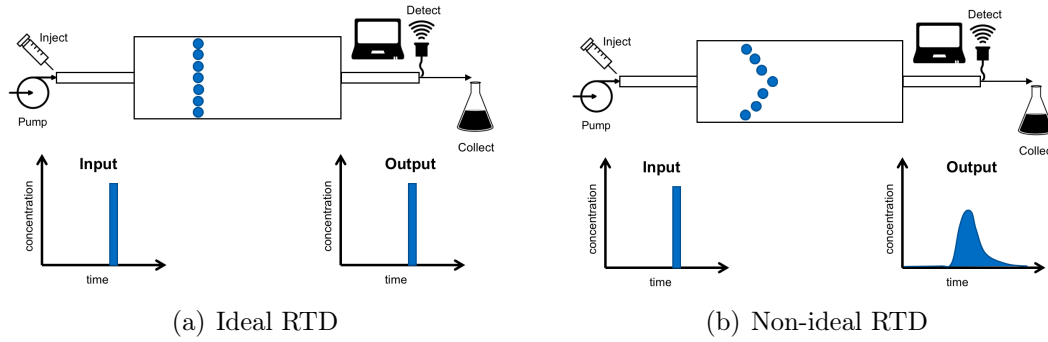


Figure 4: All molecules in reactor (a) spend the same amount of time in the reactor, so the inlet and outlet concentration plots are identical. In reactor (b), molecules spend different amounts of time due to dispersion, interactions, and imperfect mixing, creating a broader outlet peak than inlet peak.

the differential equation shown in Eqn. (5).

$$\frac{\partial C}{\partial \theta} = \left(\frac{D}{uL} \right) \frac{\partial^2 C}{\partial z^2} - \frac{\partial C}{\partial z} \quad (5)$$

As shown in Eqn. (6), the vessel dispersion number describes the ratio of diffusive effects to convective effects on the RTD and determines the shape of the RTD. Its inverse is often used, the Peclet number, Pe .

$$\text{vessel dispersion number} = \frac{1}{Pe} \equiv \frac{D}{uL} \quad (6)$$

Plotted in Fig. 5, lower dispersion numbers result in sharper RTD peaks that are closer to a sharp peak from the PFR model. Indeed, ideal reactors have sharper peaks because molecules have a high probability of spending the same time in the reactor.

The tanks-in-series method is based on the theoretical model that a PFR is an infinite series of CSTRs. Thus, a reactor with more PFR-like behavior has a higher number of CSTRs. By adding more tanks in series, the system begins to act closer to a PFR and the RTD peak sharpens as shown in Fig. 6.

$$E(\theta) = N \frac{(N\theta)^{N-1}}{(N-1)!} e^{-N\theta} \quad (7)$$

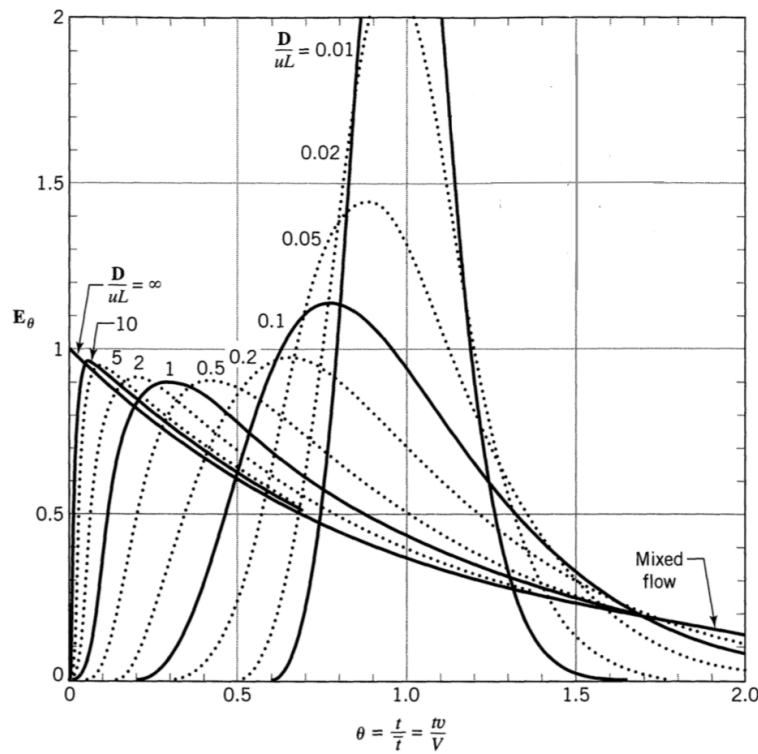


Figure 5: Residence time distributions become sharper peaks at lower vessel dispersion numbers. Low dispersion indicates plug flow-like behavior. (8)

By taking the variance of Eqn. (7), the number of TIS is calculated, as in Eqn. (8).

$$\sigma^2 = \frac{1}{N} \quad (8)$$

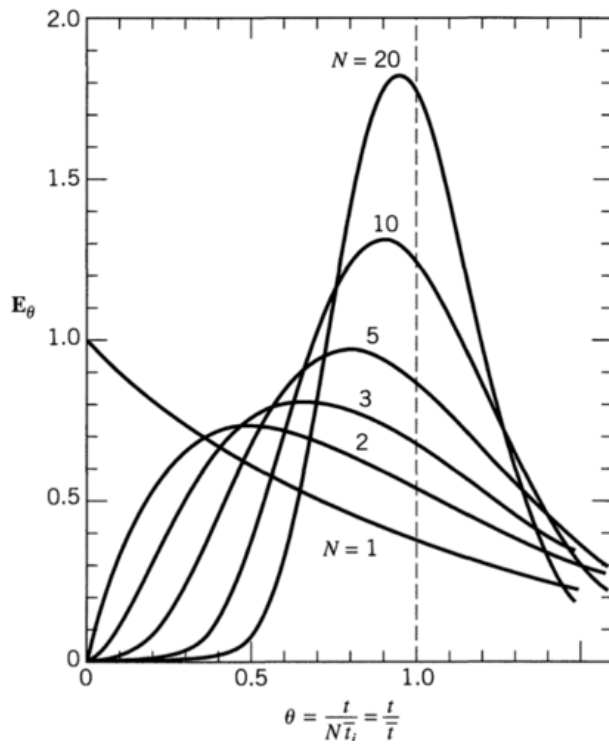


Figure 6: As more tanks are added in series, the RTD sharpens and approaches PFR behavior.

2.4 Determining Chemical Kinetics

The AFR's transparent glass reactor plates allow a user to visualize the extent of any color-changing reaction. This paper presents a new image analysis technique developed to exploit this feature. Instead of analyzing only inlet and outlet color absorbance with UV-vis spectroscopy techniques, this method and its accompanying software can quantify the extent of reaction within the AFR. A Wittig reaction (Fig. 7) was studied because of its highly visible color changes. As the reaction proceeds, the process stream changes from deeply saturated red inlet to a clear product.

There are multiple systems used to describe color quantitatively, such as RGB, CMY, and HSV colorspace, but the lattermost method was chosen to describe conversion of products in a color-changing reaction system. Using the HSV model, all resultst could be simplified down to one variable, illustrated in Fig. 8, the single-hexcone model of colorspace. Colorspace in HSV consists of three axes, hue, saturation, and value. Hue

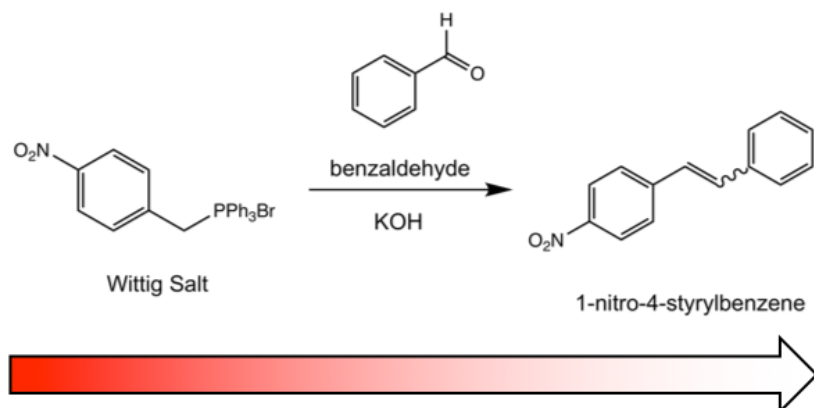


Figure 7: The Wittig intermediate reaction proceeds from a deep red to a final clear color as the Wittig salt and benzaldehyde react in the presence of base.

describes the position of a pure color on the colorwheel, saturation describes how white a color is, and the value describes the lightness or darkness of a color (9). Since absorbance of color in the Wittig reaction depends only on saturation, the S-value of a heart in any image was chosen for correlating concentration of unreacted species making the relationship between concentration and colorspace a single variable problem.

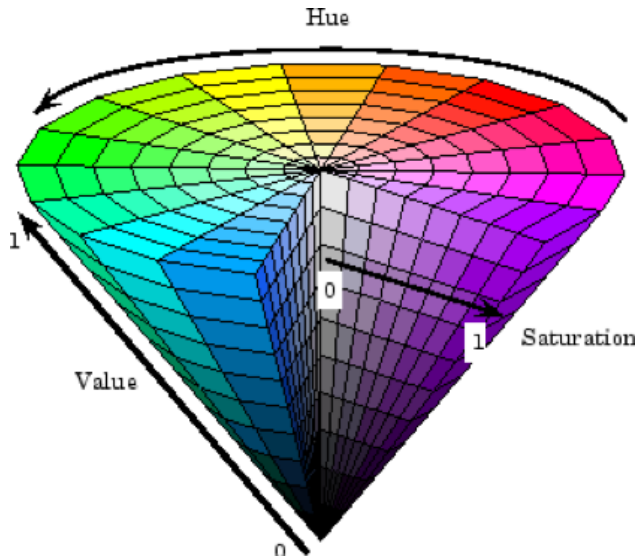


Figure 8: The single-hexcone model of colorspace for HSV suggests using saturation as a measure of color presence and thus concentration of a colored reaction system. (9)

To relate saturation of the inlet stream to a concentration, a standard curve was created. Pure reactant at varied, known dilutions was flowed through the AFR. Data was fit to a cubic equation, a standard practice in colorimetric assays where high color

saturation is present (10). Once a standard curve is known, multiple temperatures at different flowrates can be run to generate concentration versus time plots. From here, the order of reaction can be extracted with integration techniques if it is unknown.

For the pseudo-first order reaction, concentration as a function of time follows exponential decay as in Eqn. (9). The rate constant k is calculated by fitting the concentration data to this function in MATLAB using the data fitting toolbox.

$$\frac{C}{C_o} = e^{-kt} \quad (9)$$

Given the volume at which completion occurs and the volumetric flowrate required, Eqn. (10) describes the spacetime of a reaction trial which is used to find the Damkohler number (Da), a dimensionless number describing whether a reaction system is mass-transfer or kinetically limited. The Damkohler number varies with both temperature and flowrate.

$$\frac{V}{v_o} = \tau \quad (10)$$

$$Da \equiv \tau k \quad (11)$$

Further, varying temperature and measuring rate constants can be used to determine the activation energy and pre-exponential factor in the temperature-dependent Arrhenius equation,

$$k(T) = A \exp\left(-\frac{E_a}{RT}\right) \quad (12)$$

Using this workflow, kinetic parameters of a given colored-to-clear reaction can be found quickly and easily.

3 Experimental Methods

3.1 Mixing Ability of Heart-Shaped Cells

To qualitatively describe the hydrodynamic mixing ability of the AFR, blue- and yellow-dyed water (colored with methylene blue and yellow food coloring) were loaded in separate reactant containers and pumped through the system at total flowrates varying from 1.0 mL/min to 5.0 mL/min. Color changes from yellow and blue to consistent green were observed, and the location at which consistency of color was complete represented the number of hearts needed at a given flowrate to achieve full mixing.

Results of different trials were captured in high-resolution images of the reactor plates using a Nikon D5300 digital single-lens reflex camera (DSLR). These images were used to observe mixing patterns at higher magnification than possible when the reactor was operating inside the fume hood.

3.2 Effective Heat Transfer Coefficient

In order to use Eqn. (4) and determine an effective heat transfer coefficient, temperatures of the inlet and outlet polydimethyl siloxane (heat exchange fluid, HEF) and inlet and outlet process stream (water) were measured. This is possible when modeling the AFR as a parallel current heat exchanger.

Inlet HEF temperature was measured using the built-in AFR thermocouple, inlet process stream temperature was measured before the pump using a digital thermometer, outlet HEF temperature was measured with a thermocouple at the outlet heating fluid pathway, and outlet process stream temperature was measured using a thermocouple at the outlet of the reactor plate.

3.3 Residence Time Distribution of a Single Reactor Plate

Modifications of the AFR setup were necessary to include an injection and a detection point for RTD measurements. An inlet Ocean Optics DH2000-BAL 6-way pump bypass and an outlet spectrophotometer, shown schematically in Fig. 9, were added to the system. Methylene blue diluted with distilled water was injected into a 2 cm sample loop attached to the inlet pump. The pump made a single short pulse of dye into the reactor while the spectrophotometer simultaneously began absorption readings of the outlet stream. Trials were run at varying flowrates (from 1mL/min to 10 mL/min) at ambient temperature (20°C). Absorption readings of the outlet stream as a function of time were saved in Lab-View (2015) and exported to Microsoft Excel (2016) and MATLAB for analysis.

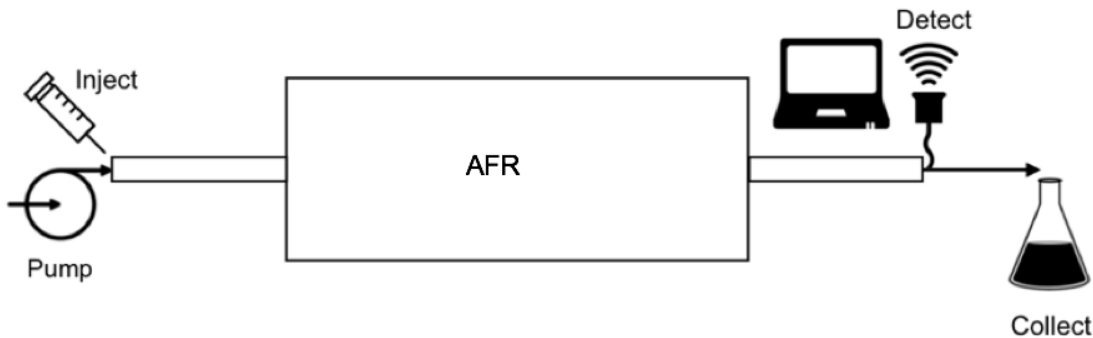


Figure 9: A schematic of the RTD collection setup. A syringe is used to inject the sample dye into a sample loop attached to the Ocean Optics DH2000-BAL six-way bypass pump before being sent through a plate of the AFR. A spectrophotometer read the outlet absorbance and stored the data in Lab View on a desktop computer. The effluent stream was collected past the detection point.

For using the dispersion model, the AFR system was characterized as an open vessel in which there are no disturbances introduced into the system other than the injection fluid. Thus, the open-open form of the age distribution, Eqn. (13), was used.

$$E_{\theta,oo} = \frac{1}{\sqrt{4\pi(D/uL)}} \exp \left[-\frac{(1-\theta)^2}{4\theta(D/uL)} \right] \quad (13)$$

Within the Jensen lab, MATLAB code was developed to fit RTD experiment results to the dispersion model distribution, Eqn. (13). The program first deconvolutes the inlet

RTD from the overall measured RTD to isolate the RTD of the reactor plate. Then the program takes initial guesses for the vessel dispersion number and residence time of the measured distribution and iterates until a best fit is reached.

A similar iterative MATLAB script was also developed in the Jensen Lab for the TIS model, Eqn. (7). This program requires exact measurements for the volumes of the inlet reactor and the AFR plate are needed as well as an initial guess of equivalent CSTRs. By iteration over the number of CSTRs, a best fit is again obtained.

3.4 Determining Chemical Kinetics

The translucent AFR plates allowed colorful reactions to be visible within the system. Using the red to clear Wittig reaction with a camera setup, image analysis techniques were developed to study temperature and flowrate effects on reaction kinetics.

First, the two reactant solutions were prepared: bromo(4-nitrobenzyl) triphenylphosphane and benzaldehylde in ethanol and potassium hydroxide in ethanol. In a 100 mL volumetric flask, 478 mg (1 mmol) 4-Nitrobenzyltriphenylphosphonium bromide was dissolved in 100 mL of ethanol. To this, 127 mg (1.2 mmol) of benzaldehyde was added and the solution was mixed thoroughly. In a second 100 mL volumetric flask, 122 mg (2.17 mmol) of potassium hydroxide was dissolved in 100 mL ethanol and allowed to dissolve for approximately 1 hour. For each solution, a pipe was inserted into the beaker and attached to a separate HPLC pump on the AFR. Temperature and total flowrate were varied between 50-100°C and 1.0-5.0 mL/min to collect a range of data points for analysis. Ranges were chosen in order to ensure the reaction completed within the first plate and were thus easily photographed.

Solutions were pumped through the AFR until steady-state was reached and the color gradient was constant. An LED mat covered with a trimmed sheet of multipurpose white 20-lb printer paper (to diffuse light) was placed behind the reactor plate to produce consistent lighting. The Nikon D5300 DSLR captured multiple images of the plate for each

trial. To maintain consistency of lighting, all of the images were captured on the same day. Uncompressed images were stored in both .raw and .jpg formats for processing in MATLAB.

The standard curve to convert saturation measurements to concentration data was produced using dilution experiments. Each dilution was produced to a total volume of 25 mL. The diluted concentrations were then loaded and pumped at a flowrate of 2.0 mL/min and at a temperature of 5°C to ensure no reaction would occur and color saturation would remain constant throughout the plate. The DSLR captured multiple images of the reactor plate for each dilution. Again, uncompressed images were stored in both .raw and .jpg formats for processing in MATLAB. The average saturation of hearts for a given dilution was fit to a cubic polynomial, creating a standard curve.

The MATLAB code created uses a fixed set of coordinates to determine the location of a heart relative to the perimeter of the plate. Using these coordinates, the saturation value is sampled from the image using a built-in HSV function in MATLAB. The user is prompted to input the temperature and flowrate before the computer plots saturation as a function of heart number. Using Eqn. (3) and the standard curve, the code produces a plot of concentration versus time. From this plot, the data is fit to an exponential curve to get the rate constant, as in Eqn. (9).

4 Results

Close-up images of the mixing experiments, shown in Fig. 10 and Fig. 11, were used to calculate mixing times and study the flow patterns at varying flowrates.



Figure 10: (Top) Yellow flowrate of 2 mL/min and blue flowrate of 2 mL/min; mixing reaches completion at the sixth heart. (Bottom) Yellow flowrate of 5 mL/min and blue flowrate of 5 mL/min; mixing reaches completion at the sixth heart. Stratifications are present at higher flowrates, indicated with arrows.

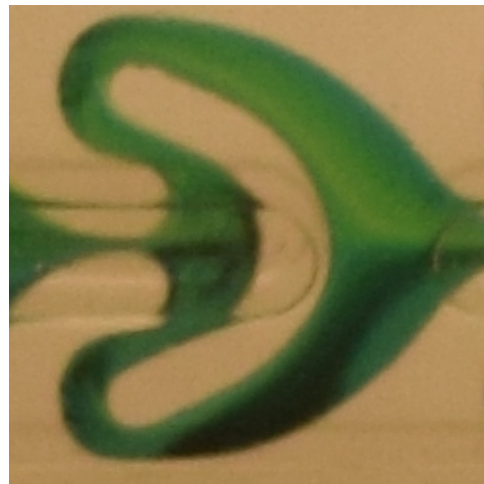


Figure 11: A closer look at a striation in Fig. 10 shows the yellow stream moving upwards around the baffle and the dark blue stream moving below the baffle. The two colors flow adjacent to one another into the next heart.

In order to model the AFR as a parallel flow heat exchanger, inlet and outlet temperatures were measured with thermocouples and presented in Table 1.

The residence time distributions were measured at nine flowrates and compared using both the tanks-in-series and dispersion methods, shown in Fig. 12 and Fig. 13.

Table 1: Inlet and outlet temperatures [°C] of AFR fluid streams were measured to calculate an effective heat transfer coefficient when modeling the system as a co-current heat exchanger.

Setpoint Temp.	HEF Temp.		Water Temp.	
	Inlet	Outlet	Inlet	Outlet
5	12.9	13.5	19.2	14.1
15	18.1	17.3	19.1	17.4
25	22.3	20.9	19.0	20.6
35	27.5	24.8	19.0	24.0
45	32.3	28.7	18.5	27.4
55	37.4	32.9	18.9	31.1
65	41.4	36.2	18.9	33.8

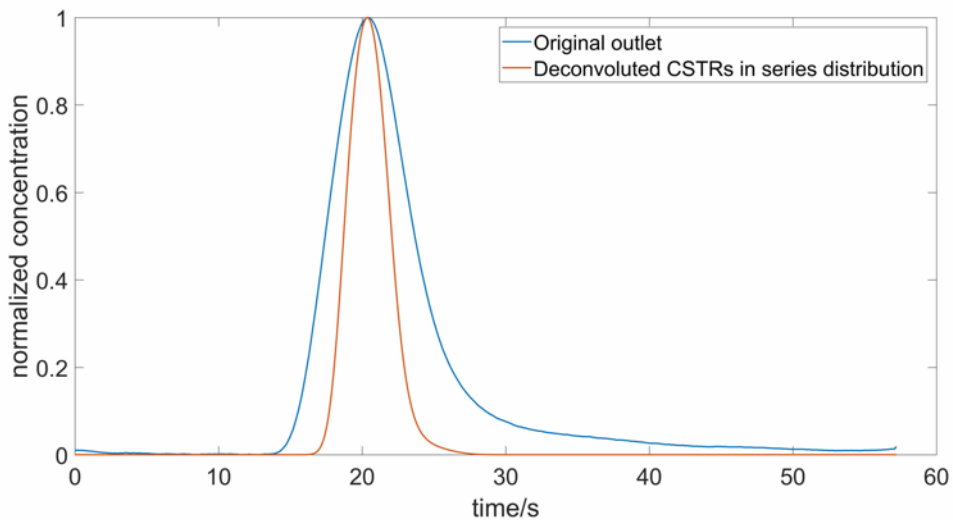


Figure 12: Before iteration to find the number of tanks in series, the RTD of the plate was extracted using deconvolution.

The dilutions of Wittig reactants (Fig. 14) were used to create a standard calibration curve shown in Fig. 15.

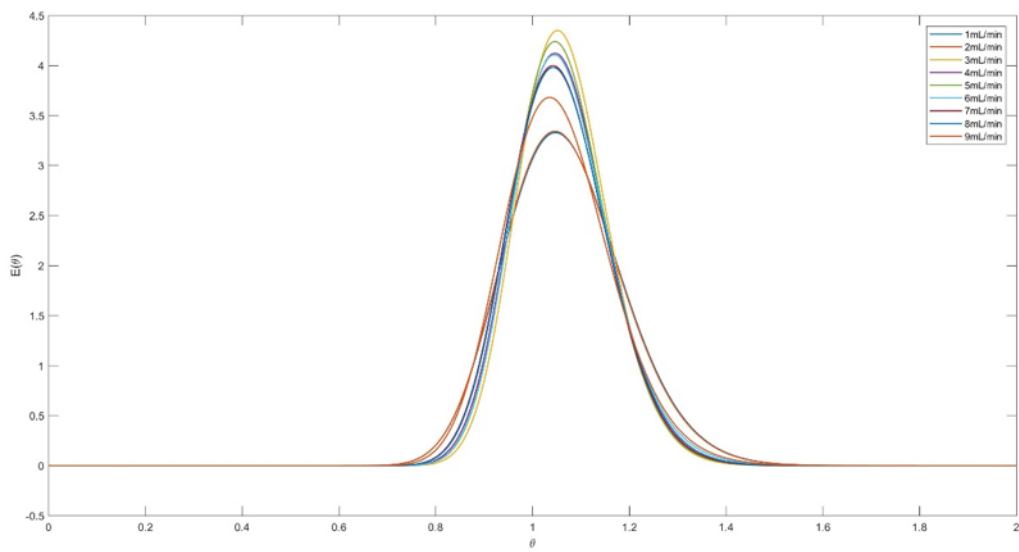


Figure 13: The various residence time distributions modeled using the dispersion method.

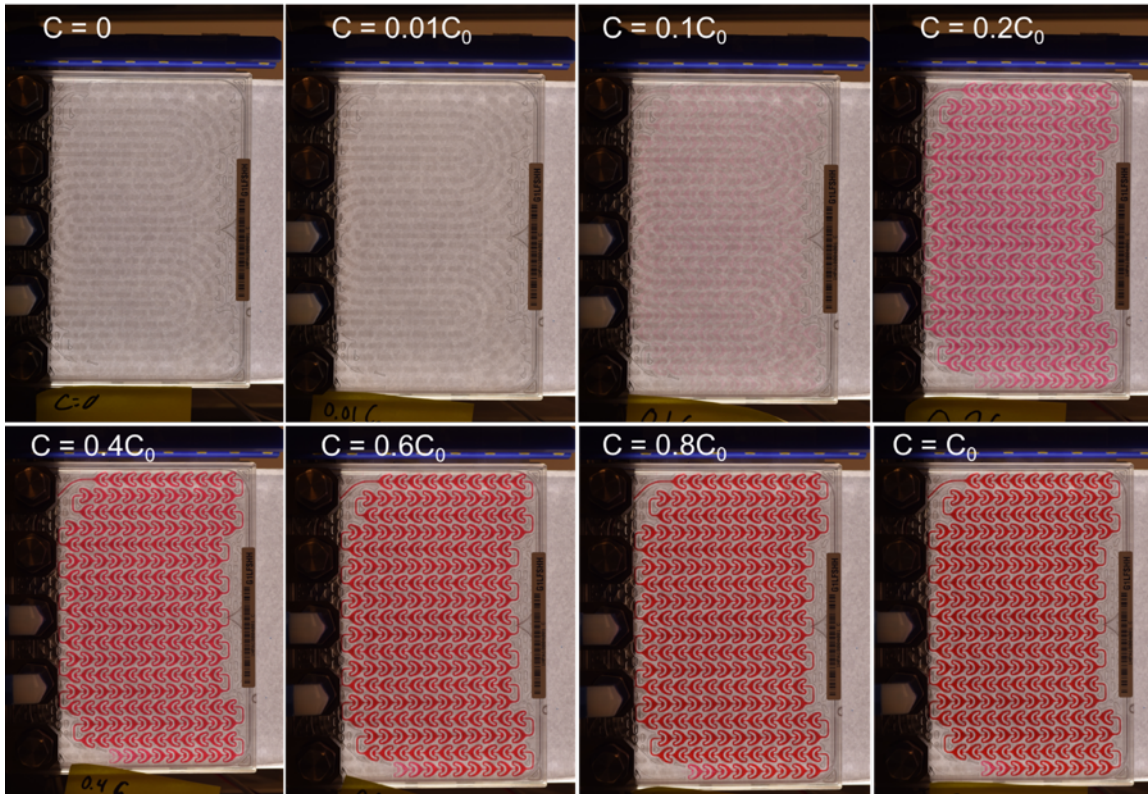


Figure 14: Wittig dilutions were carried out to create a standard curve and correlate concentration of reactant to color saturation.

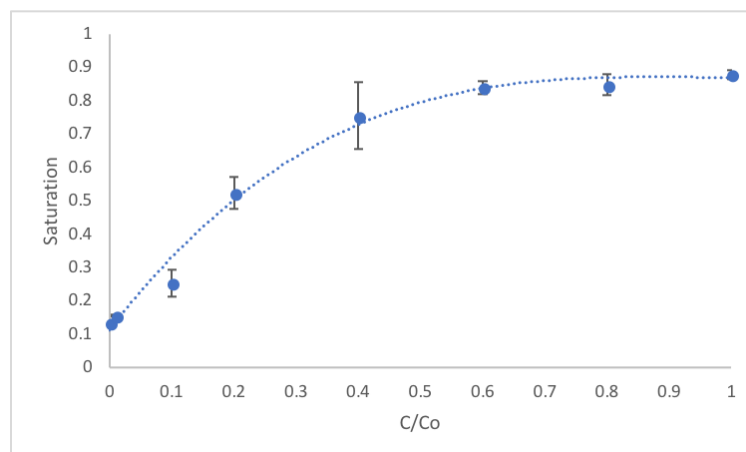


Figure 15: Samples of Wittig reactant, a dark red color, exhibited color-saturation changes at high dilutions. A cubic fit equation, Eqn. (14) was used to relate the concentration and saturation.

5 Discussion

First, characterization of the system began with simple colored-water mixing experiments. A major feature of the AFR, fast mixing benefits mass transfer since turbulent flow patterns maximize molecular contact. It was expected that time to reach complete mixing would be small based on Corning's claims. A surprising observation that higher flowrates resulted in striations of color, visible streaks of dark blue against the yellow water. This observation is likely a result of stratification of flows. Since the flow is fast along the channel, dispersion is relatively slower between the two colored flows. As seen in Table 2, mixing time was consistently fast, decreasing slightly as flowrate increased. This may be explained by a change in flow regime as fluid velocity increased.

Besides fast mixing in the reactor channels, the AFR exhibits the good heat transfer that is desired in continuous flow processes. From the measured temperatures of the inlet and outlet flows of the AFR, an effective heat transfer coefficient of $0.349 \pm 0.017 \text{ W/K}$ was determined. In comparison, the thermal conductivity of borosilicate glass is 1.09 W/mK (11). Approximating the thickness of material between the process stream of the AFR to the surroundings as 0.5 cm, the effective heat transfer coefficient of glass is $5.45 \times 10^{-3} \text{ W/K}$, which is more than 50 times smaller than the AFR. A quantitative value of the effective heat transfer coefficient of the AFR is useful for a user who wishes to check the safety of a given exothermic reaction before running it in the system.

Next, this project examined the residence time distributions (RTDs) of the AFR. The RTD plot gives insight into the non-idealities of a reactor where sharp peaks indicate

Table 2: Mixing occurs quickly, regardless of flowrate.

Total flowrate (mL/min)	Mixing time (s)
2	1.6 ± 0.41
4	1.0 ± 0.21
6	0.69 ± 0.14
8	0.67 ± 0.07
10	0.70 ± 0.07

PFR-like behavior and wide distributions indicate CSTR-like behavior. Non-idealities of a reactor deform the shape of the distribution because molecules begin to spend different amounts of time in the reactor volume. Two different models were employed in this project: the tanks-in-series (TIS) model and the dispersion model.

The average number of theoretical tanks in series using the TIS model was 72 ± 11 (Table 3), meaning the AFR behaves close to a PFR. There are limitations, however, to using the TIS model because of difficulty in capturing the tailing effect that is most visible in Fig. 12. The tailing effect refers to the dragging of the distributions, in which the distributions look skewed to the right. This illustrates that many of the particles exit the reactor much later. When using the TIS model, N , the number of equivalents tanks, was varied to best fit the experimental distributions. However, as N was varied, the distributions become more narrow. While this is since a high number of tanks lead to PFR-like behavior, the narrowing of the distributions does not capture the tailing effect which suggests the TIS model may not be appropriate to use to model the plate reactors. Furthermore, the heart cells in the reactor plate can be considered similar to theoretical tanks in series. The difference, however, is that the AFR hearts do not have powered impellers like the theoretical tanks in series would.

The dispersion method was approached as a solution to the tailing effects. Iteration, as described, was performed using MATLAB to find the vessel dispersion number, shown in Table 4. The number of tanks in series was again calculated using the variance, and the average was 107 ± 23 tanks in series. This number is higher than the TIS model and has higher error because the number of tanks in series is high and the equation becomes stiff to solve. Regardless, the results show that the reactor acts very closely like a PFR.

Finally, a promising image analysis technique was developed to analyze the kinetics of any colored-to-clear reaction run through the transparent AFR plates. A set of dilutions were created using the colored reactant. After running the fluid through the reactor and using a DSLR to capture images, the color saturation was extracted using a MATLAB

Table 3: Tanks-in-series model results show PFR behavior with large numbers of model tanks.

Flowrate (mL/min)	Number of Tanks in Series
1	82
2	82
3	54
4	63
5	67
6	66
7	67
8	76
9	90

Table 4: The dispersion model suggests PFR-like behavior as well.

Flowrate (mL/min)	Vessel Dispersion Number (10^3)	Number of Tanks in Series
1	6.81	71.5
2	6.27	77.8
3	3.68	133.8
4	3.72	132.4
5	3.94	124.9
6	3.95	124.5
7	4.65	105.6
8	4.58	107.3
9	5.35	91.5

program. The program prompts the user to crop an image of the plate and then uses a preset grid to guess the location of hearts. After checking with the user, the coordinates are then applied and transformed to fit the original image. The new coordinates are supplied to a built-in HSV function in MATLAB to gather the saturation information at the center of each heart. After averaging the saturation values and correlating to the dilution, the resulting cubic equation is shown as Eqn. (14).

$$\text{saturation} = 0.89 \left(\frac{C}{C_o} \right)^3 - 2.55 \left(\frac{C}{C_o} \right)^2 + 2.41 \left(\frac{C}{C_o} \right) + 0.11 \quad (14)$$

Using the cubic function, images of reacting systems were used to describe the concentration of species within the reactor, a task that is otherwise difficult in opaque reactors unlike the AFR. Using the image analysis setup and software, intrinsic reaction parameters like rate constants and activation energy were calculated as described previously. The image analysis techniques made possible by the transparent reactor design are a valuable tool to quickly determine kinetic parameters of any system and determine concentration at any point within the reactor plate.

From the rate constants (Table 5), it was possible to fit data to Eqn. (12) to find the activation energy and pre-exponential factor, 33.9 kJ/mol and $3.1 \times 10^4 \text{ s}^{-1}$, respectively. Using the activation energy and pre-exponential factor, it is possible to plot Da as a

Table 5: Rate constants increased with temperature.

Temperature (°C)	Rate constant (s^{-1})
35.3	0.0089 ± 0.853
42.0	0.0077 ± 0.0012
50.1	0.0098 ± 0.0013
59.2	0.0135 ± 0.0027
66.3	0.0213 ± 0.0012
77.2	0.0269 ± 0.0037
91.3	0.0421 ± 0.0039

function of temperature at various flowrates, as in Fig. 16, by using Eqn.(11) and Eqn. (12). Such a plot is useful to determine conditions where kinetic or mass transfer

limitations dominate. Knowing the flowrate and temperature at which either limitation dominates is helpful to a user of the AFR who would need to understand these operating limits.

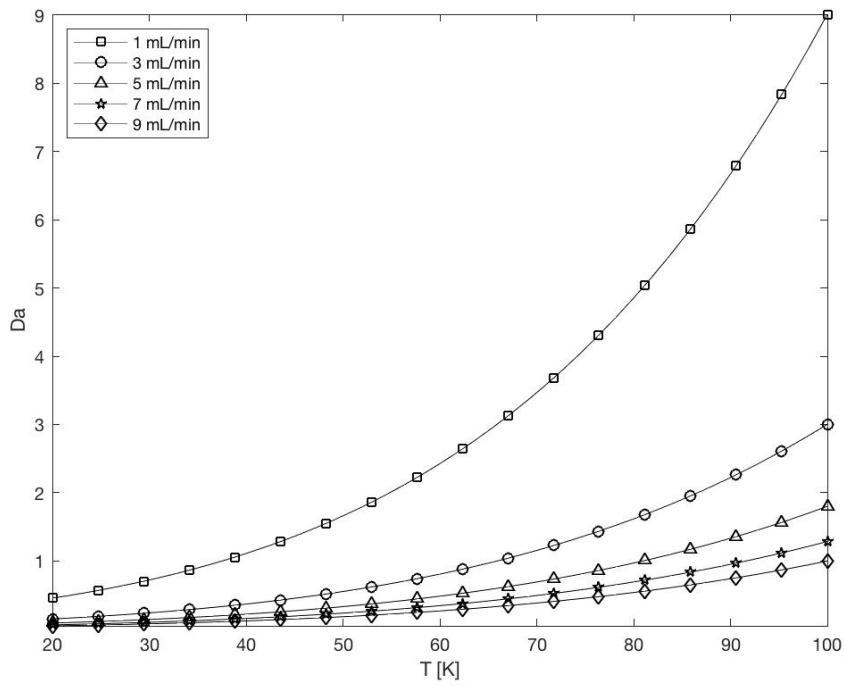


Figure 16: Damkohler number for the Wittig reaction at varying temperature and flowrates

This method of kinetic analysis was begun with a bromination reaction that proceeds from a reddish brown to clear, shown in Fig. 17. Since the color itself changed from brown to orange to yellow before clear, hue changed while saturation also changed. This two dimensional problem was not present when studying the saturation of the Wittig (because hue remained constant at red). In the future, the image analysis code may be altered to use grayscale, a possible solution because it would collapse the two dimensional hue/saturation problem down to a single variable of lightness or darkness in grayscale. Moreover, the reaction proceeded too quickly within the operating condition ranges possible in the AFR. These issues demonstrate that this technique is limited when reactions are not visible enough.

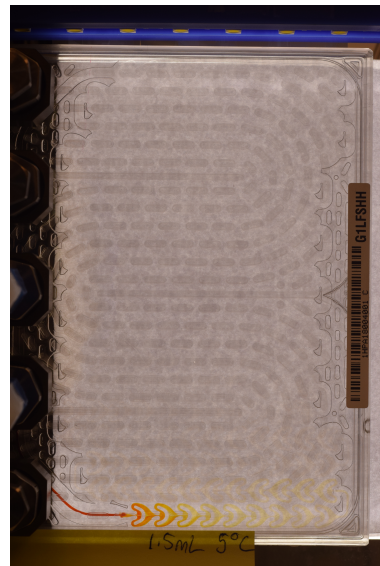


Figure 17: The bromination reaction quickly proceeds from red-brown to clear.

6 Conclusions and Recommendations

This project aimed to characterize mixing, heat transfer, and residence time distributions of the Corning AFR. In addition, an image analysis method was developed to quickly determine chemical kinetics of a given colored reaction.

From colored water tests, Corning's claims of high performance mixing in the AFR

were corroborated. A consistently mixed green colored solution consistently developed within the first row of hearts, regardless of flowrate. Striations were observed at high flowrates, an important piece of information for users who wish to understand non-idealities of fluid flow in the AFR. The effective heat transfer coefficient $0.349 \pm 0.017 \text{ W/K}$ is large in comparison to effective heat transfer coefficient of a 0.5 cm plate of borosilicate glass ($5.45 \times 10^{-3} \text{ W/K}$). From absorbance measurements of a colored dye injection into the AFR, an RTD of a reactor plate was extracted. Comparison to a tanks-in-series model revealed that a plate behaves like a series of 72 ± 11 CSTRs, a good approximation to a PFR. A better model may be the dispersion model because it captures the tailing effects seen in the measured RTD. Analysis of dispersion RTDs revealed a small vessel dispersion number of $(4.8 \pm 1.1) \times 10^3$, emphasizing the validity of a PFR assumption. To understand the reaction kinetics of the AFR, image analysis methods and tools were developed. Saturation of color and concentration of species were correlated with a standard curve. Using DSLR images of a reaction occurring at different flowrates and temperatures, activation energies and pre-exponential factors were determined for a Wittig reaction (33.9 kJ/mol and $3.1 \times 10^4 \text{ s}^{-1}$, respectively). This information can be used in the Arrhenius equation to determine the rate constant at any temperature and understand the intrinsic kinetics of the reaction in question. From there, the Damkohler number can be studied. Extending this kinetic data image analysis method to other highly visible colored-to-clear reactions is presented as a tool for AFR users wishing to exploit the benefits of transparent reactor plates. The team also would suggest, after discussions with MIT faculty during oral presentations, that calibration for colored reaction systems could be attempted using other colorspaces and with other equations (such as an exponential model instead of cubic).

In this project, work also began on a system to automatically detect the edges of every heart in the reactor plate. This method would replace the current grid mask method with a more consistent and accurate measurement of color in the reactor plate hearts. Further development to increase speed with this heart-finder program would increase productivity

in the image analysis methods proposed in this paper. After development of heart recognition and analysis software, work on automation and process control would pose interesting study. The live image analysis has potential to feed information into a control loop that could manipulate temperature or flowrate and control the product stream. For the studied reactions and a given color saturation set point, a single feedback control loop can be applied to maintain either temperature or flow rate, or a cascade feedback control scheme in which both temperature and flow rates are controlled. For example, if the color saturation was too high this would indicate the reaction had not proceeded far enough, and the image sensor would send a signal to a controller which then would increase temperature to synthesize the desired product.

This project studied a single phase system, but further research using image analysis to understand mass transfer in biphasic systems would pose interesting questions. For example, a gas-liquid carbonation experiment loaded with pH indicator would be readily studied using the software developed and presented in this paper. Understanding liquid-liquid and gas-liquid interactions in the AFR would further characterize the system.

As of the completion of this project on mixing, heat transfer, residence time distribution, and kinetic determination with image analysis, many directions of continued study are possible. Understanding the limits and benefits of using the AFR benefits future users of the system, and this project leaves open future avenues of research that can help these users.

References

- [1] Ley, S. V.; Fitzpatrick, D. E.; Ingham, R. J.; Myers, R. M. *Angewandte Chemie - International Edition* **2015**, *54*, 3449–3464.
- [2] Kaspriskie, I. *Massachusetts Institute of Technology 10.26 Project Proposal*: "Project proposal: Corning Advanced-Flow Laboratory Molecule Maker: Continuous Flow Optimization", 2018.
- [3] Schultz, V. L.; Jensen, K. F. *Massachusetts Institute of Technology 10.26 Project Introduction*: "Corning Advanced-Flow Laboratory Molecule Maker: Continuous Flow Optimization", 2018.
- [4] Plutschack, M. B.; Pieber, B.; Gilmore, K.; Seeberger, P. H. *Chemical Reviews* **2017**, *117*, 11796–11893.
- [5] Nieves-Remacha, M. J.; Kulkarni, A. A.; Jensen, K. F. *Industrial and Engineering Chemistry Research* **2012**, *51*, 16251–16262.
- [6] Corning, "Advanced Flow Reactor brochure", 2014.
- [7] Jensen, K. F. *AICHE Journal* **2017**, *63*, 858–869.
- [8] Levenspiel, O. *Chemical Reaction Engineering*; Wiley: 2 ed.; 2007.
- [9] Shipman, J. W. "The hue-saturation-value color model." <http://infohost.nmt.edu/tcc/help/pubs/colortheory/web/hsv.html>.
- [10] O'Haver, T. "Comparison of Calibration Curve Fitting Methods in Absorption Spectroscopy." <https://terpconnect.umd.edu/toh/models/BeersLawCurveFit.html>.
- [11] Perry, R.; Green, D. *Perry's Chemical Engineers' Handbook*; McGraw Hill: fifth ed.; 1973.

Appendix

Due to the large volume of images and code, all appendix materials are available freely from the team Dropbox.

Wittig kinetics image files

<https://www.dropbox.com/sh/g2ckvao3no5rt6f/AAAbERs3zz8eE82p9dejG9XSa?dl=0>

Residence time distribution deconvolution code

[https://www.dropbox.com/s/mmf6nfphwl7znla/RTD_{deconvolution}_{Ioannis}.m?dl=0](https://www.dropbox.com/s/mmf6nfphwl7znla/RTD_deconvolution_Ioannis.m?dl=0)

Image analysis code

<https://www.dropbox.com/s/kw51hk22a4kh97g/grid.m?dl=0>